UM-P-93/88

AU 9414205

Coulomb Correction Calculations of pp Bremsstrahlung

A. Katsogiannis and K. Amos

School of Physics, University of Melbourne, Parkville, 3052, Victoria, Australia

M. Jetter* and H. V. von Geramb

Theoretische Kernphysik, Universität Hamburg, Luruper Chaussee 149, D-22761 Hamburg, Germany

Abstract

The effects of the Coulomb interaction upon the photon cross section and analyzing power from pp bremsstrahlung have been studied in detail. Off-shell properties of the Coulomb T matrices have been considered but the associated, Coulomb modified, hadronic T matrices are important elements in any analysis of low energy, forward proton scattering data.

Typeset using REVTEX

I. INTRODUCTION

Nucleon–nucleon (NN) bremsstrahlung has been studied for many years [1–14] as the reaction allows a direct measure of half–off–of–the–energy–shell attributes of NN t matrices. New experimental results [15–17] as well as the specification of realistic, meson theoretic NN interactions [18,19] led to renewed interest in such bremsstrahlung [20–26] and it is now known (below pion threshold) just how photon cross sections and analyzing powers are sensitive to half–off–shell details. The importance of rescattering terms and relativistic spin corrections (RSC) in the reaction amplitudes have also been demonstrated. However, it is only recently [25] that Coulomb interaction effects in pp bremsstrahlung have been treated fully. To date, most authors either have ignored the Coulomb interaction altogether or have used a simple model in which the on–shell point particle Coulomb amplitude is added to the hadronic terms. Other authors have used the on–shell Coulomb amplitude [11,20] as a representation of these corrections. The most complete treatment in the past was made by Heller and Rich [14] who also used the Hamada–Johnston NN potential to define the hadronic interaction.

The long–range character of the Coulomb interaction makes it particularly difficult to use standard techniques of evaluation of the T matrices from the Lippmann–Schwinger equation. However, the importance of the Coulomb interaction in atomic and few body physics has produced considerable published work on the specification and application of the (pure) Coulomb off–shell T matrices [27–34] and those studies reveal ambiguities which must be treated carefully via a renormalizing procedure. So Coulomb effects need be considered and we proceed by finding solutions of inhomogeneous Schrödinger equations that result by use of the Gell-Mann–Goldberger two potential formalism [35]. This formalism is slightly different to that used by Heller and Rich [14] as they introduce Coulomb corrections by way of the total wavefunctions. The current scheme, which is presented in detail in the next section, requires evaluation of half–off–shell (pure) Coulomb T matrices and half–off–shell Coulomb modified hadronic T matrices; the latter being specified with a formalism predicated upon

the generalization of the Jost function that has been developed by Fuda and Whiting [36]. The process is no more difficult to effect than that by which the Coulomb interaction alone is considered since the short–range character of the hadronic interaction ensures no new poles arise in the development.

The pp bremsstrahlung studies reported herein extend previous ones [26] by a consistent treatment of Coulomb effects and gives more specific information than presented recently [25]. Simplified model [11,20] results are inappropriate, as will be demonstrated. Of particular interest are photon cross sections and analyzing powers for forward proton scattering angles at which it is known that the observables are sensitive to off–shell characteristics of the T matrices. This is expected to be the most important Coulomb region also due to the proximity of the outgoing protons. Further, such a study is of current relevance given the report [17] that measurements at these angles are now contemplated. Also, the limitations of the on–shell approximation for the pure Coulomb contributions due to the divergence of the on–shell Coulomb amplitude are expected to be most evident at the very forward $pp\gamma$ proton angles. The current work also includes rescattering contributions to the $pp\gamma$ transition. They are calculated in the modified soft photon approximation (MSPA) [23] and play an important role at the higher incident energies.

In Section II we introduce the Coulomb interaction into the hadronic T matrix via the two potential formalism and specify how the Coulomb corrections affect the hadronic on–shell T matrix. The fully off–shell pure Coulomb amplitude is then examined in partial wave form so that singularities are shown explicitly. Then a renormalization scheme is given to obtain the half–off–shell and on–shell Coulomb T matrix elements in the limiting case. Subsequently, the prescriptions of the half–off–shell pure Coulomb and Coulomb modified hadronic T matrix elements that are required in bremsstrahlung calculations are given explicitly and in Section III those Coulomb corrected amplitudes are used in specification of the $pp\gamma$ single scattering terms. Calculated results and a discussion of them are given in Section IV and the conclusions one may draw from this work follow in Section V.

II. DEVELOPMENT OF THE T MATRICES

In general, the T matrix operator is defined by the operator equation

$$T(K) = V\,[1 + G(K)V]\ , \tag{1}$$

where

$$G(K) = \frac{1}{K^2/2\mu - H_0 - V} \tag{2}$$

and $K^2 = 2\mu(E + i\epsilon)$. For plane wave states, $|\mathbf{k}_1\rangle$ and $|\mathbf{k}_2\rangle$, the T matrix elements are designated by

$$T_{\mathbf{k}_1\mathbf{k}_2}(K) = \langle \mathbf{k}_1|T(K)|\mathbf{k}_2\rangle \tag{3}$$

and are fully off of the energy shell when k_1 and k_2 are both different from K. Half off of the energy shell $k_2 \to K$ ($\mathbf{k}_2 = K\hat{\mathbf{k}}_2$), and in the $\epsilon \to 0$ limit, one finds

$$\begin{aligned} T_{\mathbf{k}_1\mathbf{k}_2}(k_2) &= \lim_{\epsilon\to 0}\ \langle \mathbf{k}_1|T(K)|\mathbf{k}_2\rangle \\ &= \lim_{\epsilon\to 0}\ \langle \mathbf{k}_1|V[1 + G^+(K)V]|\mathbf{k}_2\rangle \\ &= \langle \mathbf{k}_1|V|\psi^+(\mathbf{k}_2)\rangle\ , \end{aligned} \tag{4}$$

where $|\psi^+(\mathbf{k}_2)\rangle$ is the actual wavefunction solution of a particle with initial momentum $\mathbf{k}_2$ in a potential, V. It is important to note that in this formalism there is a condition on V, being that it should fall off faster than $1/r$ in the $r \to \infty$ limit. To include Coulomb effects in $pp\gamma$ calculations, it is convenient to start with the Gell-Mann–Goldberger two potential formula [35] and thus identify a Coulomb corrected hadronic T matrix, $T_{\rm HC}$, by the separation

$$T = T_{\rm C} + T_{\rm HC}\ , \tag{5}$$

where

$$T_{\rm C}(E + i\epsilon) = V_{\rm C}\,[1 + G_0(E + i\epsilon)V_{\rm C}] \tag{6}$$

and

$$T_{\rm HC}(E+i\epsilon) = [1 + V_{\rm C}G_{\rm C}(E+i\epsilon)]\, t_{\rm HC}(E+i\epsilon)\, [1 + G_{\rm C}(E+i\epsilon)V_{\rm C}] \ . \tag{7}$$

Therein $V_{\rm C} = \beta/r$ (β= constant) is the point particle Coulomb potential and the propagator with outgoing boundary conditions is

$$G_{\rm C}(E+i\epsilon) = \frac{1}{E + i\epsilon - H_0 - V_{\rm C}} \ , \tag{8}$$

when ϵ is a small positive number and H_0 is the kinetic energy Hamiltonian. The operator, $t_{\rm HC}(E+i\epsilon)$, obeys the Lippmann–Schwinger equation for the hadronic interaction ($V_{\rm H}$),

$$t_{\rm HC}(E+i\epsilon) = V_{\rm H} + V_{\rm H}G_{\rm C}(E+i\epsilon)t_{\rm HC}(E+i\epsilon) \ . \tag{9}$$

One should note that this formalism differs from the previous treatments of Coulomb effects in $pp\gamma$ calculations [11,14]. In those studies, the corrections were introduced by using the pure Coulomb r–space wavefunction, $\psi_{\rm C}$, to specify the complete nuclear wavefunction, ψ, as

$$\psi = \psi_{\rm C} + (\psi - \psi_{\rm C}) \tag{10}$$

and which is then inserted directly into the $pp\gamma$ T matrix amplitudes. As a result, what Heller and Rich refer to as the 'pure Coulomb bremsstrahlung' term is not the same as the pure Coulomb term in this study which arises from the effects of $T_{\rm C}$ alone.

A. The T Matrix On the Energy Shell

If the limit $k_1 \rightarrow k_0$ ($k_0 = k_2$) is taken in Eq. (4), then the on–shell T matrix, $T_{k_0}(\hat{\mathbf{k}}_1, \hat{\mathbf{k}}_2)$, is obtained for the momentum k_0. From formal scattering theory, this element is related to the scattering amplitude (in natural units) via

$$T_{k_0}(\theta) = \frac{-1}{4\pi^2\mu} f_{k_0}(\theta) \ , \tag{11}$$

where $\hat{\mathbf{k}}_1 \cdot \hat{\mathbf{k}}_2 = \mathrm{Cos}(\theta)$. We use this connection to study the on–shell effects to the T matrix in general. We begin with the relation between the S and T matrix,

$$S = 1 - 2\pi i T \, . \tag{12}$$

The divergence associated with the Coulomb interaction must be taken into account and we do so by using [37]

$$T = -\frac{1}{2\pi i}\{(S - S_{\mathrm{C}}) + (S_{\mathrm{C}} - 1)\} \tag{13}$$

and identifying

$$T_{\mathrm{C}} = -\frac{1}{2\pi i}(S_{\mathrm{C}} - 1) \, , \tag{14}$$

$$T_{\mathrm{I.C}} = -\frac{1}{2\pi i}(S - S_{\mathrm{C}}) \, , \tag{15}$$

since these terms are on–shell operators equivalent to those given in Eq. (5).

Taking the expectation value of the T matrix operator between initial and final plane wave states (respectively $|\mathbf{k}_2\rangle$ and $|\mathbf{k}_1\rangle$) such that $k_1 = k_0 = k_2$, then

$$[T_{\mathrm{C}}(\theta)]_{k_0} = \langle \mathbf{k}_1 | T_{\mathrm{C}} | \mathbf{k}_2 \rangle \tag{16}$$

is the on–shell Coulomb T matrix. This is related tc the Coulomb scattering amplitude (from Eq. (11)) by

$$[T_{\mathrm{C}}(\theta)]_{k_0} = \frac{-1}{4\pi^2 \mu}[f_{\mathrm{C}}(\theta)]_{k_0} \, , \tag{17}$$

where, with $V(r) = \beta/r$ and the Sommerfeld parameter, $\eta = \mu\beta/k_0$,

$$[f_{\mathrm{C}}(\theta)]_{k_0} = \frac{-\mu\beta}{2k_0^2 \sin^2(\theta/2)} e^{[2i\sigma_0 - i\eta ln[\sin^2(\theta/2)]]} \, , \tag{18}$$

and

$$e^{2i\sigma_0} = \frac{\Gamma(1 + i\eta)}{\Gamma(1 - i\eta)} \tag{19}$$

are standard Coulomb scattering quantities. Eq. (18) contains the complete Coulomb divergence so that a partial wave expansion may be used for the remaining terms in Eq. (13).

The operator, $T_{\rm HC}$, involves essentially hadronic effects only, since the pure Coulomb S matrix has been subtracted. Alternatively, as will be shown later in a discussion of its half-off-shell extension, $T_{\rm HC}$ is the hadronic T matrix but specified in the Coulomb basis. A standard partial wave decomposition of Eq. (15) which satisfies the proper asymptotic condition leads, for uncoupled channels, to the relations

$$S_{ll}^{l} = e^{2i\delta_l^l} , \qquad (S_{\rm C})_{ll}^{l} = e^{2i\sigma_l} , \tag{20}$$

where δ_l^l is the total phase shift and $\sigma_l = \arg\Gamma(l+1+i\eta)$ is the Coulomb phase shift. Due to the tensor force of the nuclear interaction there will also be coupling between the partial waves, represented by off-diagonal elements of the matrices. For coupled waves, following the Blatt-Biedenharn convention [38], the coupled S matrix is a 2×2 matrix given by

$$S_j = U_j^{-1} e^{2i\Delta_j} U_j , \tag{21}$$

where Δ_j is a diagonal matrix, U_j is a unitary matrix, with

$$S_j = \begin{pmatrix} S^j_{j-1\,j-1} & S^j_{j-1\,j+1} \\ S^j_{j+1\,j-1} & S^j_{j+1\,j+1} \end{pmatrix} ,$$

$$\Delta_j = \begin{pmatrix} e^{2i\delta_j^{j-1}} & 0 \\ 0 & e^{2i\delta_j^{j+1}} \end{pmatrix} ,$$

and

$$U_j = \begin{pmatrix} \cos\epsilon_j & \sin\epsilon_j \\ -\sin\epsilon_j & \cos\epsilon_j \end{pmatrix} . \tag{22}$$

ϵ_j is the coupling parameter and $\delta_j^{l=j\pm1}$ are the upper and lower phase shifts respectively, when there is no coupling ($\epsilon_j \to 0$).

It is desirable to express the total phase shifts, δ_j^l, in terms of the Coulomb (σ_l) and nuclear, $(\delta_H)_j^l$, phase shifts; the latter being obtained from the solutions of the Lippmann-Schwinger equations excluding Coulomb effects. This is possible if two approximations hold

[37]. First, the Coulomb interaction must be essentially required only outside of the nuclear region and, second, the WKB approximation must be valid in this outside region. Then the full phase shifts may be expressed as

$$\delta_j^l = (\delta_H)_j^l + \sigma_l \ . \tag{23}$$

In terms of the T matrix elements, via Eq. (15) for uncoupled channels, one finds

$$\begin{aligned}(T_{\rm HC})_{ll}^l &= \frac{1}{2ik_0}(e^{2i\delta_l^l} - e^{2i\sigma_l}) \\ &= \frac{1}{2ik_0}(e^{2i(\delta_H)_l^l} - 1)e^{2i\sigma_l} \\ &= (T_{\rm H})_{ll}^l e^{2i\sigma_l} \ . \end{aligned} \tag{24}$$

The coupled on-shell T matrix elements are obtained similarly if the relation between the coupled S matrix, from Eq. (21), for both interactions (S_j) and nuclear interaction alone ($(S_{\rm H})_j$) is given by

$$S_j = e^{i\Sigma_j}(S_{\rm H})_j e^{i\Sigma_j} \ , \tag{25}$$

and

$$\Sigma_j = \begin{pmatrix} \sigma_{j-1} & 0 \\ 0 & \sigma_{j+1} \end{pmatrix} \ , \tag{26}$$

where σ_{j-1} and σ_{j+1} represent the lower and upper coupled channel Coulomb phase shifts respectively. Eq. (21) gives the forms of the S_j, $(S_{\rm C})_j$, and $(S_{\rm H})_j$ elements. The nuclear interaction obeys the hadronic equivalent of Eq. (14) and along with Eq. (15) the partial wave expressions are

$$(T_{\rm H})_{l'l}^j = \frac{1}{2ik_0}\{(S_{\rm H})_{l'l}^j - \delta_{l'l}\} \ , \tag{27}$$

$$(T_{\rm HC})_{l'l}^j = \frac{1}{2ik_0}\{S_{l'l}^j - (S_{\rm C})_{l'l}^j\} \ , \tag{28}$$

where $\delta_{l'l}$ is the Kronecker delta. The equations are slightly more complicated than in the uncoupled case but it is reasonably straightforward to show, if the elements of Eq. (25) are rearranged to match Eqs. (27) and (28), that

$$(T_{\rm HC})^{j}_{j\pm1\ j\pm1} = e^{2i\sigma_{j\pm1}}(T_{\rm H})^{j}_{j\pm1\ j\pm1}\ ,$$

$$(T_{\rm HC})^{j}_{j\pm1\ j\mp1} = e^{i(\sigma_{j\pm1}+\sigma_{j\mp1})}(T_{\rm H})^{j}_{j\pm1\ j\mp1}\ . \tag{29}$$

From Eqs. (17), (24), and (29) it is evident that the on-shell effect of including the Coulomb interaction in derivation of the complete NN T matrix is to add the on-shell Coulomb T matrix, $[T_{\rm C}(\theta)]_{k_0}$, to the sum of the partial wave hadronic T matrix elements, which are rotated by the Coulomb phase shifts in the complex plane.

B. Off-Shell Properties of the Pure Coulomb T Matrices

The half-off-shell properties of the two proton T matrices are required to analyze $pp\gamma$ data. To define those properties however, we must begin with the fully off-shell forms (Eq. (3)) to identify the pole structure that is introduced by inclusion of Coulomb effects.

Consider first the pure Coulomb operator, $T_{\rm C}$. Dušek [33] has made a partial wave expansion of its amplitude and has studied the associated poles extensively. In momentum space, as there are no coupled states for the pure Coulomb interaction, one may write [39] (units in which $\hbar = 2\mu = 1$ are used hereafter)

$$\langle k_1|[T_{\rm C}(K)]_l|k_2\rangle = \frac{2K\eta}{\pi k_1 k_2}\int_0^1 {\rm d}t\, t^{i\eta}\frac{\rm d}{{\rm d}t}Q_l(z(t))\ , \tag{30}$$

in which Q_l is a Legendre function of the second kind and now (recalling that $K^2 = 2\mu(E+i\epsilon)$ here)

$$\eta = \mu\beta/K\ , \tag{31}$$

and

$$z(t) = \frac{1}{2k_1k_2}\left\{k_1^2+k_2^2-\frac{(1-t)^2}{t}\frac{(k_1^2-K^2)(k_2^2-K^2)}{K^2}\right\}\ . \tag{32}$$

The small imaginary part of η in the $t^{i\eta}$ term allows the singularities of these integrals to be handled, when the Coulomb interaction is given by

$$V_C(r) = \lim_{\epsilon \to 0} \frac{2K\eta}{r} \,. \tag{33}$$

Foregoing the details of the calculation, Dušek [33] derived the expression

$$\begin{aligned}\langle k_1|[T_C(K)]_l|k_2\rangle = & \frac{iK}{\pi k_1 k_2}\Gamma^2(1-i\eta)\frac{\Gamma(l+1+i\eta)}{\Gamma(l+1-i\eta)}e^{-\eta\pi}\frac{\mathcal{P}_l(A,-i\eta)}{(k_1+K)^{2i\eta}}\frac{\mathcal{P}_l(A',-i\eta)}{(k_2+K)^{i\eta}} \\ & \times(k_1^2-E-i\epsilon)^{i\eta}(k_2^2-E-i\epsilon)^{i\eta} - \frac{iK}{\pi k_1 k_2}\Gamma(1+i\eta)\Gamma(1-i\eta) \\ & \times\mathcal{P}_l(A,i\eta)\mathcal{P}_l(A',-i\eta)\left(\frac{k_1+K}{k_2+K}\right)^{2i\eta}\left(-\frac{k_2^2-E-i\epsilon}{k_1^2-E-i\epsilon}\right)^{i\eta} \\ & +\{\mathcal{F}_C(k_1,k_2,K;i\eta)\}_l + \{\mathcal{G}_C(k_1,k_2,K;i\eta)\}_l \,. \end{aligned} \tag{34}$$

Therein

$$A = \frac{k_1^2+K}{2k_1K} \,, \qquad\qquad A' = \frac{k_2^2+K}{2k_2K} \,, \tag{35}$$

and

$$\mathcal{P}_l(x,\alpha) = P_l^{(-\alpha,\alpha)}(x)/P_l^{(-\alpha,\alpha)}(1) \,, \tag{36}$$

involves the Jacobi polynomials, $P_l^{(\alpha,\beta)}(x)$. $(\mathcal{F}_C)_l$ and $(\mathcal{G}_C)_l$ are functions similar to the leading terms in Eq. (34) and have been separated as they have a special property in the half-off-shell limit, namely that

$$\lim_{k_2 \to K}\{\mathcal{F}_C(k_1,k_2,K;i\eta)\}_l = 0 \tag{37}$$

and for $k_1 \neq K$,

$$\lim_{k_2 \to K}\{\mathcal{G}_C(k_1,k_2,K;i\eta)\}_l = 0 \,. \tag{38}$$

Defining the on-shell momentum, k_0, as

$$k_0 = \lim_{\epsilon \to 0} K \ , \tag{39}$$

and setting $k_2 = k_0$, then

$$\lim_{\epsilon \to 0} \{\mathcal{F}_C(k_1, k_0, K; i\eta)\}_l = 0 \tag{40}$$

and for $k_1 \neq K$,

$$\lim_{\epsilon \to 0} \{\mathcal{G}_C(k_1, k_0, K; i\eta)\}_l = 0 \ . \tag{41}$$

With these results, taking the limit $k_2 \rightarrow k_0$ in Eq. (34) shows that the element $\langle k_1 | [T_C(K)]_l | k_0 \rangle$ oscillates due to the on-shell Coulomb singularities. A renormalization procedure [30,33] is required to obtain the conventional half-off-shell Coulomb amplitudes, which are given by

$$\lim_{\epsilon \to 0} \frac{\langle k_1 | [T_C(K)]_l | k_0 \rangle}{\Gamma(1 - i\eta) \left(\frac{\epsilon}{4k_0^2}\right)^{i\eta}} = \langle k_1 | [T_C(k_0)]_l | k_0 \rangle_{\rm LIM} \ . \tag{42}$$

Therein 'LIM' means that amplitude is only defined strictly in the limit and not by the simple substitution $k_2 = k_0$. The half-off-shell pure Coulomb T matrix elements are then

$$\langle k_1 | [T_C(k_0)]_l | k_0 \rangle_{\rm LIM} = i \frac{e^{-\frac{1}{2}\eta\pi}}{\pi k_1} \Bigg\{ \Gamma(1 - i\eta) \frac{\Gamma(l + 1 + i\eta)}{\Gamma(l + 1 - i\eta)} \mathcal{P}_l(A, -i\eta) \frac{(k_1^2 - k_0^2)^{i\eta}}{(k_1 + k_0)^{2i\eta}}$$

$$- \Gamma(1 + i\eta) \mathcal{P}_l(A, i\eta) \frac{(k_1 + k_0)^{2i\eta}}{(k_1^2 - k_0^2)^{i\eta}} \Bigg\} \ ; \tag{43}$$

a result that can be obtained also by expressing the half-off-shell T matrix in terms of off-shell Jost functions [33,40]. As there is no restriction on l in this development and as the normalization factor is independent of the partial wave value, the result holds for the complete pure Coulomb T matrix amplitude. However, in the absence of an alternative derivation, there are still ambiguities as to what is the correct Coulomb half-off-shell T matrix. We choose the conventional form [29], which follows from Eq. (43). This point shall be pursued later, when we consider this amplitude in analytic form.

The on-shell limit of Eq. (43) has been shown [33] to be

$$\{(T_C)_{k_0}\}_l = \lim_{k_1 \to k_0} \frac{1}{\Gamma(1-i\eta)} \left(i\frac{k_1^2 - k_0^2}{4k_0^2} \right)^{-i\eta} \left\{ \langle k_1 | [T_C(k_0)]_l | k_0 \rangle \right.$$

$$\left. + i\frac{e^{-\frac{1}{2}\eta\pi}}{\pi k_1}\Gamma(1+i\eta)\mathcal{P}_l(A, i\eta)\frac{(k_1+k_0)^{2i\eta}}{(k_1^2-k_0^2)^{i\eta}} \right\} , \tag{44}$$

and to which we seek to equate from Eq. (17),

$$\{(T_C)_{k_0}\}_l = -\frac{2}{\pi}\{(f_C)_{k_0}\}_l = -\frac{2}{\pi}\frac{1}{2ik_0}\frac{\Gamma(l+1+i\eta)}{\Gamma(l+1-i\eta)} \tag{45}$$

the known partial wave on-shell Coulomb T matrix elements. Note should be taken that the inclusion of the second term in Eqs. (43) and (44) is necessary only for the specific partial waves and equates to zero in the summation for the complete T_C matrix element.

C. The T Matrix Half Off the Energy Shell

1. Specification of the Half-Off- and On-Shell T Matrices

We have interactions of the form

$$V = V_H + V_C \tag{46}$$

where V_H converges faster than $1/r$ asymptotically so that all of the poles of the total T matrix are contained in T_C and the development leading to Eqs. (42) and (44) can be generalized in terms of the complete operator, T. We have, therefore, the partial wave summed results

$$\lim_{\epsilon \to 0} \frac{\langle \mathbf{k}_1 | T(K) | \mathbf{k}_0 \rangle}{\Gamma(1-i\eta)\left(\frac{\epsilon}{4k_0^2}\right)^{i\eta}} = \langle \mathbf{k}_1 | T(k_0) | \mathbf{k}_0 \rangle_{\mathrm{LIM}} \tag{47}$$

and

$$\lim_{k_1 \to k_0} \frac{\langle \mathbf{k}_1 | T(k_0) | \mathbf{k}_0 \rangle}{\Gamma(1-i\eta)\left(i\frac{k_1^2-k_0^2}{4k_0^2}\right)^{i\eta}} = T_{k_0}(\theta) . \tag{48}$$

For the T_{HC} components, a partial wave decomposition can be used without ambiguity and hadronic channel coupling can be included by conventional expansions [26]. Specifically, with Eqs. (4), (7), (47), and (48), one finds

$$\lim_{\epsilon\to 0}\frac{\langle k_1|[T_{\rm HC}(K)]^j_{l'l}|k_0\rangle}{\Gamma(1-i\eta)\left(\frac{\epsilon}{4k_0^2}\right)^{i\eta}} = {}_{\rm C}\langle k_1,k_0-,l'|[t_{\rm HC}(k_0)]^j_{l'l}|k_0,k_0+,l\rangle_{\rm C} \tag{49}$$

and

$$\lim_{k_1\to k_0}\frac{{}_{\rm C}\langle k_1,k_0-,l'|[t_{\rm HC}(k_0)]^j_{l'l}|k_0,k_0+,l\rangle_{\rm C}}{\Gamma(1-i\eta)\left(i\frac{k_1^2-k_0^2}{4k_0^2}\right)^{i\eta}} = {}_{\rm C}\langle k_0,k_0-,l'|[t_{\rm HC}(k_0)]^j_{l'l}|k_0,k_0+,l\rangle_{\rm C}\ , \tag{50}$$

where $|k_1,k_0+,l\rangle_{\rm C}$ are the outgoing half–off–shell partial Coulomb waves given by

$$|k_1,k_0+,l\rangle_{\rm C} = \lim_{\epsilon\to 0}\frac{|k_1,k_0^2+i\epsilon,l\rangle_{\rm C}}{\Gamma(1-i\eta)\left(\frac{\epsilon}{4k_0^2}\right)^{i\eta}} \tag{51}$$

and

$$|k_1,k_0^2+i\epsilon,l\rangle_{\rm C} = [1+\{G_{\rm C}(k_0^2+i\epsilon)\}_l(V_{\rm C})_l]|k_1,l\rangle \tag{52}$$

with $|k_1,l\rangle$ being the plane partial waves. Hence, after renormalization, the half–off– and on–shell $T_{\rm HC}$ amplitudes are defined by the corresponding Lippmann–Schwinger operator solution, $t_{\rm HC}$, taken between Coulomb wavefunctions. Considering the form of Eq. (9), they are defined as Coulomb corrected hadronic T matrix elements.

2. Evaluation of the Half–Off–Shell Amplitudes

The half–off–shell pure Coulomb T matrix may be obtained as a three dimensional analytic expression; the desired form for practical purposes because of the slow convergence of the pure Coulomb partial wave series. That results by casting Eq. (47) into an equivalent form of Eq. (4), namely

$$[T_{\rm C}(k_0)]_{\mathbf{k}_1\mathbf{k}_0} = \langle\mathbf{k}_1|T_{\rm C}(k_0)|\mathbf{k}_0\rangle_{\rm LIM} = \langle\mathbf{k}_1|V_{\rm C}|\psi^+_{\rm C}(\mathbf{k}_0)\rangle_{\rm LIM}\ ; \tag{53}$$

the wavefunction of which is most readily defined in r–space as

$$\psi^+_{\rm C}(\mathbf{r}) = \frac{1}{(2\pi)^{\frac{3}{2}}}e^{-\eta\pi/2}e^{i\mathbf{k}\cdot\mathbf{r}}\Gamma(1+i\eta)_1F_1[-i\eta,1,i(kr-\mathbf{k}\cdot\mathbf{r})]\ . \tag{54}$$

Substituting this into the right hand side of Eq. (53) gives

$$[T_C(k_0)]_{\mathbf{k}_1\mathbf{k}_0} = \frac{\beta}{(2\pi)^3} e^{-\eta\pi/2}\Gamma(1+i\eta)\int \frac{d\mathbf{r}}{r} e^{i(\mathbf{k}_0-\mathbf{k}_1)\cdot\mathbf{r}}\, {}_1F_1[-i\eta, 1, i(k_0 r - \mathbf{k}_0\cdot\mathbf{r})] \,. \tag{55}$$

A contour integration method [41] may be used to evaluate these integrals. Such is shown in detail in Appendix (7.1) of Ref. [29], and the result is

$$[T_C(k_0)]_{\mathbf{k}_1\mathbf{k}_0} = \frac{\beta}{2\pi^2} e^{-\eta\pi/2}\Gamma(1+i\eta) \lim_{\lambda\to 0^+} \frac{\{k_1^2 - (k_0+i\lambda)^2\}^{i\eta}}{\{(\mathbf{k}_1-\mathbf{k}_0)^2+\lambda^2\}^{1+i\eta}} \,. \tag{56}$$

Taking this amplitude on the energy shell ($k_1 = k_0$) gives a scattering amplitude

$$\begin{aligned}[f_C(\theta)]' &= -4\pi^2\mu[T_C(k_0)]_{\mathbf{k}_1\mathbf{k}_0}|_{k_1=k_0} \\ &= \lim_{\lambda\to 0^+} f_C(\theta)\{\Gamma(1-i\eta)e^{-i\eta\ln(2k/\lambda)}\} \,, \end{aligned} \tag{57}$$

where $f_C(\theta)$ is the conventional Coulomb scattering amplitude. Thus, Eq. (53) does not lead to the correct answer on-shell, and the result also depends on the limiting process used (*e.g.* $\lambda \to 0$ then $k_1 \to k_0$). This discontinuity was first noted by Okubo and Feldman [42] and Ford [27] confirmed its existence. Furthermore, the parameter λ in Eq. (56) represents a screening of the Coulomb potential that is required as, on the energy shell, asymptotic contributions are important and the long range Coulomb effects are strongest. This is consistent with the forward scattering divergence of the amplitude $f_C(\theta)$. We note, as an aside, that Ford has shown [28], by using the cut-off Coulomb potential,

$$V(r) = \begin{cases} \beta/r, & \text{if } r < R \\ 0, & \text{if } r > R \end{cases} \,, \tag{58}$$

in the $R \to \infty$ limit the limiting process is unimportant and the correct off-shell T_C matrix is given in all cases, except for when any two of the momenta (k_0, k_1, k_2) are equal. There are ambiguities as to what is the correct half-off-shell expression for the Coulomb T matrix. A meaningful definition, however, is to use Eq. (56) to represent the amplitude, in accordance with Eq. (43) and the half-off-shell discontinuity is given by

$$|[T_C(k_0)]_{\mathbf{k}_1\mathbf{k}_0}| = \frac{\beta}{2\pi^2}\frac{1}{(\mathbf{k}_1-\mathbf{k}_0)^2} \begin{cases} e^{-\eta\pi/2}|\Gamma(1+i\eta)|, & \text{if } k_1 > k_0 \\ 1, & \text{if } \kappa_1 = k_0 \\ e^{\eta\pi/2}|\Gamma(1+i\eta)|, & \text{if } k_1 < k_0 \end{cases} \,. \tag{59}$$

As noted by Ford [27], the long–range of the Coulomb potential distorts the incident and scattered waves at infinity, and thus Eq. (53) is not strictly correct for the Coulomb interaction. However, as this distortion is relatively weak, use of Eq. (53) is a good approximation.

As the $T_{\rm HC}$ amplitude contains no singularities for short–range hadronic potentials, $V_{\rm H}$, then the $T_{\rm HC}$ part of Eq. (47) can be substituted directly into Eq. (4) for the half–off–shell T matrix, as per Eq. (49). Using the Coulomb interaction in the Lippmann–Schwinger equation poses major numerical problems. However, stable solutions have been obtained recently [43] whereby partial wave momentum space matrix elements of the Coulomb modified hadronic interaction can be evaluated using a mixed representation. Nevertheless, we proceed in r–space and begin with Eq. (9) and

$$t_{\rm H}(E+i\epsilon) = V_{\rm H} + V_{\rm H} G_0(E+i\epsilon) t_{\rm H}(E+i\epsilon)\,, \tag{60}$$

where

$$G_0(E+i\epsilon) = \frac{1}{(E+i\epsilon) - H_0} \tag{61}$$

is the free Green's operator. Wave operators, $\Omega_0(E+i\epsilon)$ and $\Omega_{\rm C}(E+i\epsilon)$, are defined [44] by

$$\Omega_0(E+i\epsilon) = 1 + G_0(E+i\epsilon) t_{\rm H}(E+i\epsilon) \tag{62}$$

and

$$\Omega_{\rm C}(E+i\epsilon) = 1 + G_{\rm C}(E+i\epsilon) t_{\rm HC}(E+i\epsilon)\,, \tag{63}$$

so that Eqs. (60) and (9) may be rewritten as

$$t_{\rm H}(E+i\epsilon) = V_{\rm H}\Omega_0(E+i\epsilon) \tag{64}$$

and

$$t_{\rm HC}(E+i\epsilon) = V_{\rm H}\Omega_{\rm C}(E+i\epsilon)\,, \tag{65}$$

respectively. Substituting Eq. (64) into Eq. (62) leads to

$$\{E + i\epsilon - H_0 - V_{\rm H}\}\Omega_0(E + i\epsilon) = E + i\epsilon - H_0 \tag{66}$$

and likewise, substituting Eq. (65) in Eq. (63) yields

$$\{E + i\epsilon - H_0 - V_{\rm C} - V_{\rm H}\}\Omega_{\rm C}(E + i\epsilon) = E + i\epsilon - H_0 - V_{\rm C}\,. \tag{67}$$

Tensor coupling in the nuclear interaction means that matrix elements of these operators are to be taken between eigenfunctions of the total angular momentum, j, and a mixed representation is introduced such that for plane waves with momentum magnitude q one has

$$\langle \mathbf{r}|q, lsjm_j\rangle = \sqrt{\frac{2}{\pi}} j_l(qr)\mathcal{Y}^{m_j}_{lsj}(\hat{\mathbf{r}})\,, \tag{68}$$

in which $j_l(qr)$ are the regular spherical Bessel functions and $\mathcal{Y}^{m_j}_{lsj}(\hat{\mathbf{r}})$ are the usual tensor spherical harmonics,

$$\mathcal{Y}^{m_j}_{lsj}(\hat{\mathbf{r}}) = \sum_{\mu\nu}\langle ls\mu\nu|jm_j\rangle Y_{l\mu}(\hat{\mathbf{r}})|s\nu\rangle\,. \tag{69}$$

Eq. (66) then becomes

$$\{E + i\epsilon - \nabla^2 - V_{\rm H}\}\langle \mathbf{r}|\Omega_0(E + i\epsilon)|k_1, l'sjm_j\rangle = (E + i\epsilon - k_1^2)\sqrt{\frac{2}{\pi}} j_{l'}(k_1 r)\mathcal{Y}^{m_j}_{l'sj}(\hat{\mathbf{r}}) \tag{70}$$

for which k_1 is a general momentum magnitude in units of $\hbar^2/2\mu$; μ is the reduced proton mass. In this representation the Coulomb waves are given by

$$\langle \mathbf{r}|q, lsjm_j\rangle_{\rm C} = \sqrt{\frac{2}{\pi}}\frac{F_l(qr)}{qr}\mathcal{Y}^{m_j}_{lsj}(\hat{\mathbf{r}})\,, \tag{71}$$

where $F_l(qr)$ are the regular Coulomb functions, and Eq. (67) is given by

$$\{E + i\epsilon - \nabla^2 - (V_{\rm C} + V_{\rm H})\}\langle \mathbf{r}|\Omega_{\rm C}(E + i\epsilon)|k_1, l'sjm_j\rangle_{\rm C} = (E + i\epsilon - k_1^2 - V_{\rm C})\sqrt{\frac{2}{\pi}}\frac{F_{l'}(k_1 r)}{k_1 r}\mathcal{Y}^{m_j}_{l'sj}(\hat{\mathbf{r}})\,. \tag{72}$$

Eqs. (62) and (63) can now be written as

$$\langle \mathbf{r}|\Omega_0(E+i\epsilon)|k_1,l'sjm_j\rangle = \sqrt{\frac{2}{\pi}} j_{l'}(k_1 r)\mathcal{Y}^{m_j}_{l's_j}(\hat{\mathbf{r}}) + \int d\mathbf{r}'\langle \mathbf{r}|G_0(E+i\epsilon)|\mathbf{r}'\rangle\langle \mathbf{r}'|t_{\rm H}(E+i\epsilon)|k_1,l'sjm_j\rangle \tag{73}$$

and

$$\langle \mathbf{r}|\Omega_{\rm C}(E+i\epsilon)|k_1,l'sjm_j\rangle_{\rm C} = \sqrt{\frac{2}{\pi}}\frac{F_{l'}(k_1 r)}{k_1 r}\mathcal{Y}^{m_j}_{l's_j}(\hat{\mathbf{r}}) + \int d\mathbf{r}'\langle \mathbf{r}|G_{\rm C}(E+i\epsilon)|\mathbf{r}'\rangle\langle \mathbf{r}'|t_{\rm H}(E+i\epsilon)|k_1,l'sjm_j\rangle_{\rm C}\,, \tag{74}$$

respectively. The asymptotic boundary conditions in each case are carried in the Green's functions so that in the limit $\epsilon \to 0$

$$\langle \mathbf{r}|G_0^+(k_0)|\mathbf{r}'\rangle = -k_0\sum_{lm} j_l(k_0 r_<)h_l^+(k_0 r_>)Y_{lm}(\hat{\mathbf{r}})Y^*_{lm}(\hat{\mathbf{r}}')\,, \tag{75}$$

where $h_l(z)$ is a spherical hankel function, and

$$\langle \mathbf{r}|G_{\rm C}^+(k_0)|\mathbf{r}'\rangle = -k_0\sum_{lm}\frac{F_l(k_0 r_<)}{k_0 r}\frac{H_l^+(k_0 r_>)}{k_0 r}Y_{lm}(\hat{\mathbf{r}})Y^*_{lm}(\hat{\mathbf{r}}')\,, \tag{76}$$

where

$$H_l^{\pm}(z) = G_l(z) \pm iF_l(z)\,, \tag{77}$$

in which $G_l(z)$ are the irregular Coulomb solutions. Using the properties of the spherical Bessel functions and Eq. (68) one can show that Eq. (73) asymptotes to

$$\lim_{r\to\infty}\langle \mathbf{r}|\Omega_0^+(k_0)|k_1,l'sjm_j\rangle = \sqrt{\frac{2}{\pi}}\frac{1}{k_1 r}\sum_l\{\sin(k_1 r - \frac{1}{2}l'\pi)\delta_{l'l} + k_1\langle k_0,lsjm_j|t_{\rm H}^+|k_1,l'sjm_j\rangle e^{i(k_0 r-\frac{1}{2}l\pi)}\}\mathcal{Y}^{m_j}_{ls_j}(\hat{\mathbf{r}})\,. \tag{78}$$

A similar result is derived from Eq. (74) with the replacement of the argument,

$$qr \to qr - \eta \ln(2qr), \tag{79}$$

and is

$$\lim_{r\to\infty} \langle \mathbf{r}|\Omega_{\rm C}^{+}(k_0)|k_1, l'sjm_j\rangle_{\rm C} = \sqrt{\frac{2}{\pi}}\frac{1}{k_1 r}\sum_l \{\sin(k_1 r - \eta' \ln(2k_1 r) - \frac{1}{2}l'\pi)\delta_{l'l} + k_1\, {}_{\rm C}\langle k_0, lsjm_j|t_{\rm HC}^{+}|k_1, l'sjm_j\rangle_{\rm C} \times e^{i(k_0 r - \eta \ln(2k_0 r) - \frac{1}{2}l\pi)}\} \mathcal{Y}_{lsj}^{m_j}(\hat{\mathbf{r}}) \,, \tag{80}$$

where $\eta' = \mu\beta/k_1$. Defining

$$\langle k_0, lsjm_j|t_{\rm H}^{+}|k_1, l'sjm_j\rangle \equiv \{t_{\rm H}^{+}(k_0, k_1; k_0)\}_{ll'}^{jst} \tag{81}$$

and

$${}_{\rm C}\langle k_0, lsjm_j|t_{\rm HC}^{+}|k_1, l'sjm_j\rangle_{\rm C} \equiv \{t_{\rm HC}^{+}(k_0, k_1; k_0)\}_{ll'}^{jst} \,, \tag{82}$$

time reversal invariance then gives

$$\{t^{+}(k_0, k_1; k_0)\}_{ll'}^{jst} = \{t^{+}(k_1, k_0; k_0)\}_{l'l}^{jst} \,, \tag{83}$$

so that Eq. (82) is equivalent to Eq. (49). Thus, the half–off–shell elements of $t_{\rm HC}$ can be obtained from the asymptotic solutions given in Eq. (80). Note that the substitution $k_1 = k_0$ therein gives the correct on–shell t matrix elements.

Solutions of Eqs. (70) and (72) involve the ansatz

$$\langle \mathbf{r}|\Omega^{+}(k_0)|k_1, l'sjm_j\rangle = \sqrt{\frac{2}{\pi}}\frac{1}{k_1 r}\sum_l \phi_{l'l}(k_0, k_1, r)\mathcal{Y}_{lsj}^{m_j}(\hat{\mathbf{r}}) \tag{84}$$

in accordance with the asymptotic form of Eqs. (78) and (80), and substituting this in Eqs. (70) and (72) yields the radial equations

$$\left\{\frac{\mathrm{d}^2}{\mathrm{d}r^2} + k_0^2 - \frac{l(l+1)}{r^2} - V_{\rm H}\right\}\phi_{l'l} = (k_0^2 - k_1^2)u_l(k_1 r)\delta_{l'l} \,, \tag{85}$$

where $u_l(z) = z j_l(z)$ are the Riccati–Bessel functions, and

$$\left\{\frac{\mathrm{d}^2}{\mathrm{d}r^2}+k_0^2-\frac{l(l+1)}{r^2}-(V_{\mathrm{C}}+V_{\mathrm{H}})\right\}\phi_{l'l}=(k_0^2-k_1^2-V_{\mathrm{C}})F_l(k_1r)\delta_{l'l}\,. \tag{86}$$

Thus to determine the hadronic half–off–shell t matrix elements, with or without Coulomb corrections, a procedure similar to that of the usual matching problem for the on–shell t matrix can be used. Essentially the only difference is that the Schrödinger equation now contains an inhomogeneous term. Alternatively the half–off–shell elements of t_{H} and t_{HC} may be obtained [36] from the small r behaviour of the off–shell Jost solutions, $f_l(k_0,k_1,r)$. Considering uncoupled channels for simplicity, one has with this alternate scheme

$$\{t^+(k_1,k_0;k_0)\}_l=\left(\frac{k_0}{k_1}\right)^l\frac{f_l(k_0,k_1)-f_l(k_0,-k_1)}{\pi i k_1 f_l(k_0,k_0)}\,, \tag{87}$$

where

$$f_l(k_0,k_1)=\frac{k_1^l e^{-il\pi/2}(2l+1)}{(2l+1)!!}\lim_{r\to 0}r^l f_l(k_0,k_1,r)\,. \tag{88}$$

The $f_l(k_0,k_1,r)$ are solutions of the equations

$$\left\{\frac{\mathrm{d}^2}{\mathrm{d}r^2}+k_0^2-\frac{l(l+1)}{r^2}-V_{\mathrm{H}}\right\}f_l(k_0,k_1,r)=(k_0^2-k_1^2)e^{il\pi/2}w_l^+(k_1r)\,, \tag{89}$$

in which $w_l^{\pm}(z)$ are Riccati–Neumann functions. The solutions of Eq. (89) are constrained to have the asymptotic forms

$$f_l(k_0,k_1,r)\underset{r\to\infty}{\longrightarrow}e^{ik_1r}\,. \tag{90}$$

Clearly for $k_1=\pm k_0$, these are the irregular solutions of the Schrödinger equation, given by the Jost solution, $f_l(\pm k_0,r)=f_l(k_0,\pm k_0,r)$. For the Coulomb modified solutions, one merely makes the replacements $w_l^+(k_1r)\to H_l^+(k_1r)$ in Eq. (89) (where $H_l^+(z)$ is defined by Eq. (77)) and $k_1r\to k_1r-\eta\ln(2k_1r)$ in Eq. (90).

III. INCLUSION OF THE T MATRICES IN THE PROTON–PROTON BREMSSTRAHLUNG CALCULATION

To develop the complete $pp\gamma$ $\mathcal{T}$ matrix amplitude, the Gell-Mann–Goldberger two potential formalism [35] is used with the electromagnetic interaction, V_{em}, and the nuclear T matrix operator. Therewith, the total bremsstrahlung transition operator, $\mathcal{T}$, is given by

$$\mathcal{T} = V_{\rm em} + [T^-(E_f)]^\dagger G^+(E_f) V_{\rm em} + V_{\rm em} G^+(E_i) T^+(E_i)$$
$$+ [T^-(E_f)]^\dagger G^+(E_f) V_{\rm em} G^+(E_i) T^+(E_i) \ , \tag{91}$$

in which the indices i and f refer to initial and final proton states respectively, the (-) and (+) superscripts refer to incoming and outgoing boundary conditions respectively, E is the energy of the two protons, and $G(E)$ are the propagators for the protons. As the leading term represents radiation by a free particle, it does not contribute to calculations. The second and third entries are the single scattering terms while the last is the rescattering term.

In the current work the rescattering term is calculated using the modified soft photon approximation (MSPA) [23] in order to simplify the numerical integration. Extensions have been made to second order in the rescattering spin correction terms [45]. The pure Coulomb (T_C) amplitudes are very small for the energy domain in which the rescattering term becomes relevant and have been neglected. However, the more important Coulomb corrected hadronic T matrix has been included by direct substitution ($T_H \rightarrow T_{HC}$) in the rescattering amplitude and thus leaves the formal expressions unchanged.

As developed, the Coulomb interaction enters the nuclear T matrix as per Eq. (5). The total $\mathcal{T}$ matrix elements are to be constructed with the relative motion proton states $|\mathbf{p}, S, M\rangle$ and photon states $|\mathbf{k}\rangle$, with $\mathbf{p}$, S, and M being relative proton momentum, total spin, and spin projection, respectively, while $\mathbf{k}$ is the photon momentum. Using subscripts 1 and 2 to represent the incoming protons and the primed subscripts for the outgoing protons, the amplitude from the single scattering terms is

$$\langle S'M' | \mathcal{T}_{\rm single} | SM \rangle =$$

$$\sum_{S''M''} \left\{ \frac{\langle S''M'', \frac{1}{2}(\mathbf{p}_1 - \mathbf{p}_2 - \mathbf{k}) | T^-(E_f) | \frac{1}{2}(\mathbf{p}_1' - \mathbf{p}_2'), S'M' \rangle^* \times \langle S''M'' | V_{\rm em}^{(1)} | SM \rangle}{(E_f - E_{\mathbf{p}_1 - \mathbf{k}} - E_{\mathbf{p}_2})} \right.$$

$$\left. + \frac{\langle S''M'', \frac{1}{2}(\mathbf{p}_1 - \mathbf{p}_2 + \mathbf{k}) | T^-(E_f) | \frac{1}{2}(\mathbf{p}_1' - \mathbf{p}_2'), S'M' \rangle^* \times \langle S''M'' | V_{\rm em}^{(2)} | SM \rangle}{(E_f - E_{\mathbf{p}_1} - E_{\mathbf{p}_2 - \mathbf{k}})} \right.$$

$$+\frac{\langle S'M'|V_{\rm em}^{(1)'}|S''M''\rangle \times \langle S''M'', \frac{1}{2}(\mathbf{p}_1' - \mathbf{p}_2' + \mathbf{k})|T^+(E_i)|\frac{1}{2}(\mathbf{p}_1 - \mathbf{p}_2), SM\rangle}{(E_i - E_{\mathbf{p}_1'+\mathbf{k}} - E_{\mathbf{p}_2'})}$$

$$+\frac{\langle S'M'|V_{\rm em}^{(2)'}|S''M''\rangle \times \langle S''M'', \frac{1}{2}(\mathbf{p}_1' - \mathbf{p}_2' - \mathbf{k})|T^+(E_i)|\frac{1}{2}(\mathbf{p}_1 - \mathbf{p}_2), SM\rangle}{(E_i - E_{\mathbf{p}_1'} - E_{\mathbf{p}_2'+\mathbf{k}})}\Bigg\} \tag{92}$$

in which the energies are $E_{\mathbf{p}} = \sqrt{(\mathbf{pc})^2 + (mc^2)^2}$. Two forms of nuclear T matrix elements,

$$\langle S'M', \mathbf{p}'|T^+(E_{\mathbf{p}})|\mathbf{p}, SM\rangle \tag{93}$$

and

$$\langle S'M', \mathbf{p}'|T^-(E_{\mathbf{p}})|\mathbf{p}, SM\rangle^* \tag{94}$$

enter according to whether the initial or final state is on-shell. Parity conservation and the antisymmetry of the wavefunction restrict them to having no singlet–triplet transitions, whence $S' = S$.

We substitute Eq. (5) in these amplitudes and make partial wave decompositions of the $T_{\rm HC}$ components, *viz.*

$$\langle s\nu', \mathbf{p}'|[T_{\rm HC}(E_{\mathbf{p}})]^{\pm}|\mathbf{p}, s\nu\rangle = \frac{4}{\pi}\sum_{\substack{jll'm_j m_l m_{l'} \\ (s+l+1\ \text{odd})}} i^{l-l'}\,[T_{\rm HC}(p', p; E_{\mathbf{p}})]_{l'l}^{jst=1\,\pm}$$
$$\times \langle lsm_l\nu|jm_j\rangle\langle l'sm_{l'}\nu'|jm_j\rangle Y_{lm_l}^*(\hat{\mathbf{p}})Y_{l'm_{l'}}(\hat{\mathbf{p}}')\,, \tag{95}$$

in which the equations are antisymmetrized. The partial wave amplitude boundary conditions are related via

$$\{[T(p', p; E_{\mathbf{p}})]_{l'l}^{jst-}\}^* = [T(p', p; E_{\mathbf{p}})]_{l'l}^{jst+} \tag{96}$$

so both elements (Eqs. (93) and (94)) are given by $[T_{\rm HC}(p', p; E_{\mathbf{p}})]_{l'l}^{jst=1\,+}$. For the pure Coulomb amplitudes, antisymmetrization gives

$$\langle SM'|T_C^{\pm}(E_{\mathbf{p}})|SM\rangle = \{[T_C(p)]^{\pm}_{\mathbf{p}'\mathbf{p}} + (-1)^S[T_C(p)]^{\pm}_{\mathbf{p}'-\mathbf{p}}\}\delta_{M'M} \tag{97}$$

for the half–off–shell case, where $[T_C(p)]^{+}_{\mathbf{p}'\mathbf{p}}$ is given by Eq. (56), and

$$\langle SM'|T_C^{\pm}(E_{\mathbf{p}})|SM\rangle = \{[T_C(\theta)]^{\pm}_{p} + (-1)^{\cdot}[T_C(\pi-\theta)]^{\pm}_{p}\}\delta_{M'M} \tag{98}$$

for the on–shell case, where $[T_C(\theta)]^{+}_{p}$ is given by Eq. (17).

In order to evaluate the observables for the four nuclear amplitudes in Eq. (92), the z–axis may be taken to lie along the incident beam, $\hat{\mathbf{p}}$, and subsequently each matrix element rotated from its individual reference frame to the overall $pp\gamma$ CM frame with quantization along a chosen single axis. However, inclusion of the rescattering term in the MSPA makes it most convenient to use Eq. (95) and thus to avoid rotating the amplitudes.

IV. RESULTS AND DISCUSSION

In all of the calculations, the results of which are presented herein, all single scattering amplitudes, the rescattering terms, relativistic spin corrections (RSC), and exact half–off–shell T matrices derived from the Paris interaction [18] have been used. The centre of momentum frame of reference (CM) has been used in these evaluations whence the rescattering terms, being proportional to the CM momentum to leading order, are smallest.

To demonstrate the role of Coulomb forces in calculations of pp bremsstrahlung, we compare the results of four model prescriptions. The complete calculations based upon the theoretical development given in Section II C, and so including the exact half–off–shell Coulomb and the half–off–shell Coulomb modified hadronic (two proton) T matrices, gave the results designated hereafter by 'full Coulomb'. The results found from calculations as detailed above but with the free hadronic t matrices (solutions of the Lippmann–Schwinger equation) are identified by the label 'simple Coulomb'. A third set of calculations were made with no Coulomb effects taken into account at all and are identified by 'no Coulomb'. Finally, we have made calculations using the approximation proposed by Workman and Fearing [20] which is a 'simple Coulomb' calculation but with the pure Coulomb T matrices

themselves taken to be on the energy shell. The results of this fourth type of calculation are denoted by 'on-shell Coulomb' and are described by Eqs. (17), (24) and (29).

Calculations of the photon angular distribution cross section and analyzing powers (A_y) have been made using the coplanar, symmetric geometries with the specific proton scattering angles (30°, 30°), (12°, 12°), and (5°, 5°) or a similar geometry when data was available. The measurables have been calculated for incident energies of 5, 42, 157, and 280 MeV, and are presented in Figs. 1, 2, 3 and 5 respectively. In these diagrams the 'full Coulomb', 'no Coulomb', 'simple Coulomb', and 'on-shell Coulomb' results are displayed by the solid, dotted, dashed, and dot-dashed curves respectively. Also, with cross sections given in the left hand and analyzing powers in the right hand panels, the 5°, 12°, and 30° proton angle cases are displayed in the bottom, middle, and top segments respectively.

The 5 MeV results are given in Fig. 1 from which it is evident that the 'full Coulomb' cross sections have a typical electric quadrupole shape [26] but are approximately one half the size of the very similar results of the 'no Coulomb' and 'simple Coulomb' calculations. Obviously the major Coulomb contributions come from the correction to the hadronic T matrix at all proton angles. But the 'on-shell Coulomb' result is sizeably different as the proton angle decreases and has already become invalid by (12°, 12°), growing worse at more forward angles. The divergence is not evident in the 5° cross section graph as it is two orders of magnitude larger in scale. This reflects the on-shell divergence of the pure Coulomb T matrices for forward scattering. It is also noted that our results are markedly larger at the forward proton angles than comparable ones found by Heller and Rich [14], which we attribute to their use of the Hamada-Johnston interaction.

The analyzing power results shown in Fig. 1 are singularly uninspiring. With the exception of the erroneous 'on-shell Coulomb' result at small proton angles, the analyzing powers are unlikely to be measurably different from zero. Nevertheless the cross section magnitude strongly reflects the Coulomb modification of the NN t matrices from their 'no Coulomb' values.

The results obtained with an incident energy of 42 MeV are displayed in Fig. 2. For

the largest proton angle (30°), the Coulomb effects have become irrelevant. All four model calculations yield cross sections which are essentially indistinguishable. The discrepancies with the data noted by Workman and Fearing [20] for these coplanar geometries at 42 MeV are obviously not resolved by inclusion of the Coulomb and rescattering correction terms but are rather due to the binning and resolution errors described in Ref. [46]. The associated analyzing powers are likewise indistinguishable for (30°, 30°) but at the other angles, the differences between the 'full Coulomb', 'no Coulomb', and 'simple Coulomb' model results are noticeable, although quite reduced in comparison to the 5 MeV case. At the smaller proton angles the 'on–shell Coulomb' result again diverges markedly. The lesser importance of the Coulomb effects makes this approximation a better one than at 5 MeV but it is still too poor at (12°, 12°). The analyzing powers are not sufficiently different, it seems, for such measurements to be able to discriminate between the other three model calculations. Nevertheless, at 42 MeV as well, it is important to treat the Coulomb effects properly as the gross 'on–shell Coulomb' calculation remains very problematic for proton scattering angles below $\sim 20°$.

The 157 MeV results are shown in Fig. 3. As noted previously [26], the magnetic component of the electromagnetic transition operator becomes more important with increasing energy and is dominant especially for forward proton scattering. This is evident from the change in qualitative behaviour of the cross section at the forward proton angles. The cross section barely distinguishes any Coulomb contributions and the 'on–shell Coulomb' calculation is vastly improved compared to the (12°, 12°) at 42 MeV. The analyzing powers now have distinctive and measurable magnitudes that increase markedly for forward proton scattering. The decreasing importance of the Coulomb interaction with increasing energy for $pp\gamma$ competes with the growth of A_y at the forward proton angles. Quantitatively, the largest Coulomb effects to the analyzing power occur at roughly 160 MeV and (5°, 5°). The 'full Coulomb', 'no Coulomb', and 'simple Coulomb' results are all very similar and are quite different from the 'on–shell Coulomb' model result. In sum though the specific Coulomb effects are quite small at this energy and furthermore, the (5°, 5°) cross section becomes

quite featureless and contains little discriminatory information, in contrast to A_y. The rapid decrease in the Coulomb effects coincides with the suppression of contribution from the $^1S_0$ two nucleon channel. This is apparent from simple kinematical considerations. In general, the bremsstrahlung amplitude is dominated by the process in which the photon is emitted before the strong interaction (first two terms in Eq. (92)). These nuclear T matrices are on the energy shell for the relative momentum of the two outgoing protons $p' = \frac{1}{2}|\mathbf{p}'_1 - \mathbf{p}'_2|$. For a given incident energy, this quantity is small at forward proton angles and photon emissions near the incident axis. Thus the relative S-wave contribution of the amplitude and the magnitude of the pure Coulomb T matrix (Eq. (56)) are enhanced. Moreover, the hadronic Coulomb correction is also increased at small p' and, particularly for the S-channel,

$$\lim_{q\to 0} T_{HC}(q, p'; E_{\mathbf{p}'}) = \lim_{p'\to 0} T_{HC}(q, p'; E_{\mathbf{p}'}) = 0 \tag{99}$$

whereas the pure hadronic $^1S_0$ T matrix remains finite for small on-shell and off-shell momenta. Consequently, the Coulomb barrier *reduces* the hadronic S-wave amplitude at small momenta; the effect of the hadronic Coulomb correction is *destructive* in kinematic situations characterized by small p' and S-wave dominance. This can clearly be seen from the cross sections in Fig. 1 and the (12°,12°) and (5°,5°) diagrams of Fig. 2.

The magnetic transitions of the singlet channels are also very weak whence the variation (with proton angle) of cross sections from typical electric quadrupole to magnetic dipole character is consistent with the other observations of $^1S_0$ channel suppression [26].

The cross section data shown in Fig. 3 were measured with a noncoplanar acceptance angle, $\bar{\phi}$, of 0 to 1° in the 'Harvard Noncoplanar Geometry' [13]. In Fig. 4, the 'full Coulomb' cross sections we find from calculations using the coplanar (0°), mid-range (0.5°), and limit (1°) values of that acceptance are compared with the data. These results are displayed by the solid, dashed, and dotted curves respectively. Clearly the current data set does not distinguish readily between those results although the χ^2 per data point values are 1.94, 1.79, and 2.00 respectively. Also shown, by the dot-dashed curve, is the cross section one obtains when the rescattering corrections are omitted from the otherwise 'full Coulomb' $\bar{\phi} = 0.5°$,

noncoplanar calculation. This curve gives a χ^2 per data point fit of 2.67 specifically.

By energies near pion threshold, the Coulomb effects are hardly essential to predict either cross sections or analyzing powers. This is evident in Fig. 5 wherein the 280 MeV results are displayed. Again the 'on-shell Coulomb' model fails abysmally at the very forward proton scattering angles (of 5°) but the notable feature is the improvement of that model calculation to the point where, for (12°, 12°), the divergence is not yet dominating the total $\mathcal{T}$ matrix amplitude. This is also evident for the analyzing powers with data shown from the (14°, 12.4°) TRIUMF measurement. All model calculations provide a good fit to the data. Shown in Fig. 6 are four calculations for the 280 MeV (14°, 12.4°) analyzing power, A_y, wherein the 'full Coulomb' result is given by the solid curve and the same calculation but excluding rescattering contributions is given by the dashed line. The dot-dashed and dotted curves shown therein are the results of the complete 'on-shell Coulomb' calculation and the same calculation without rescattering, respectively. The latter is the model used by Workman and Fearing [20] and lies closer to the 'full Coulomb' curve than the dashed line although addition of the rescattering terms alters the result markedly at the forward photon angles. The exact treatment of Coulomb effects is slightly less important at this energy and geometry than the inclusion of rescattering contributions.

Finally the energy variation of the 5° proton cross section and analyzing power is shown in Fig. 7. Only the 'full Coulomb' results are shown with the different energy cases identified by the solid, dashed, dotted, and dot-dashed curves for the 5, 42, 157, and 280 MeV values respectively. The cross sections reveal the trend from electric quadrupole to magnetic dipole character with increasing energy. The energy variation in the 20°-30° photon angle region grows from 0.1 to 0.4 μb/sr^2/rad over this range and as such could be easily discerned by measurement. The same angular range gives observable changes with the analyzing power, although this observable becomes appreciable in size only for energies in excess of 100 MeV.

Physically, the small sensitivity of the $pp\gamma$ reaction observables to the Coulomb interaction at higher energies reflects the closer approach of the colliding protons in the process. For a given geometry, the Coulomb effect to the $pp\gamma$ observables becomes less important with

increasing energy of the projectile. On the other hand, if the energy is fixed, Coulomb effects are enhanced at forward proton angles, i. e. in the region of small p', large photon momenta, and thus large off-shell effects. For energies near pion threshold, however, Coulomb effects are relatively small even for the analyzing power in the extreme off-shell domain.

V. CONCLUSIONS

The purpose of this study was to define and assess, as fully as possible, the effects of the Coulomb interaction in pp bremsstrahlung. To this end, we defined the two proton Coulomb t matrices half off of the energy shell and their hadronic t matrices in a Coulomb basis as is required from use of the Gell-Mann-Goldberger two potential formalism. Those t matrices were used in the single scattering terms for $pp\gamma$. Our 'full Coulomb' calculations also included RSC and rescattering terms. With the latter, as we evaluated transition amplitudes defined in the CM frame, Coulomb effects are expected to be small and were ignored. Coplanar, symmetric scattering was considered in particular.

The proper treatment of Coulomb effects is most important at low energies and for forward proton scattering. At the lowest energy considered (5 MeV), the full calculation gave cross sections that were half the size of those found without Coulomb effects or with a simple model approximation to them. With increasing energy, the cross sections varied to those characteristic of magnetic interaction dominance and the specific differences due to Coulomb effects diminished. At pion threshold, where the $^1S_0$ two proton channel is least important, the cross sections are essentially independent of the inclusion of Coulomb terms. But the on-shell approximation for Coulomb amplitudes is very poor at all energies due to its forward scattering divergence. The analyzing power is less revealing of exact Coulomb effects since at low energies all results are extremely small in magnitude. It is unlikely that experiments could discriminate between our full results and those found with no Coulomb effects at all.

REFERENCES

* Present Address: TRIUMF, 4004 Wesbrook Mall, Vancouver, British Columbia, Canada, V6T 2A3.

[1] M. I. Sobel and A. H. Cromer, Phys. Rev. **132**, 2698 (1963).

[2] I. Slaus, J. W. Verba, J. R. Richardson, R. F. Carlson, W. T. H. van Oers, and L. S. August, Phys. Rev. Lett. **17**, 536 (1966).

[3] A. H. Cromer and M. I. Sobel, Phys. Rev. **152**, 1351 (1966); *Erratum*, Phys. Rev. **152**, 1385 (1966).

[4] K. W. Rothe, P. F. M. Koehler, and E. H. Thorndike, Phys. Rev. **157**, 1247 (1967).

[5] V. R. Brown, Phys. Lett. **25B**, 506 (1967).

[6] W. A. Pearce, W. A. Gale, and I. M. Duck, Nucl. Phys. **B3**, 241 (1967).

[7] B. Gottschalk, W. J. Schlaer, and K. H. Wang, Nucl. Phys. **A94**, 491 (1967).

[8] M. L. Halbert, D. L. Mason, and L. C. Northcliffe, Phys. Rev. **168**, 1130 (1968).

[9] D. Drechsel and L. C. Maximon, Ann. Phys. (N.Y.) **49**, 403 (1968).

[10] V. R. Brown, Phys. Rev. **177**, 1498 (1969).

[11] D. Marker and P. Signell, Phys. Rev. **185**, 1286 (1969).

[12] M. K. Liou and K. S. Cho, Nucl. Phys. **A124**, 85 (1969).

[13] M. K. Liou and M. I. Sobel, Ann. Phys. (N.Y.) **72**, 323 (1972).

[14] L. Heller and M. Rich, Phys. Rev. C **10**, 479 (1974).

[15] P. Kitching *et al*, Nucl. Phys. **A463**, 87c (1987).

[16] K. Michaelian *et al*, Phys. Rev. D **41**, 2689 (1990).

[17] B. v. Przewoski, H. O. Meyer, H. Nann, P. V. Pancella, S. F. Pate, R. E. Pollock, T. Rinckel, M. A. Ross, F. Sperisen, Phys. Rev. C **45**, 2001 (1992).

[18] M. Lacombe, B. Loiseau, J. M. Richard, R. Vinh Mau, J. Côté, P. Pirès, R. de Tourreil, Phys. Rev. C **21**, 861 (1980).

[19] R. Machleidt, K. Holinde, and Ch. Elster, Phys. Rep. **149**, 1 (1987).

[20] R. L. Workman and H. W. Fearing, Phys. Rev. C **34**, 780 (1986).

[21] K. Nakayama, Phys. Rev. C **39**, 1475 (1989).

[22] V. Herrmann and K. Nakayama, Phys. Rev. C **44**, R1254 (1991); V. Herrmann and K. Nakayama, Phys. Rev. C **45**, 1450 (1992); H. W. Fearing, Nucl. Phys. **A463**, 95c (1987).

[23] V. Herrmann, J. Speth, and K. Nakayama, Phys. Rev. C **43**, 394 (1991).

[24] V. R. Brown, P. L. Anthony, and J. Franklin, Phys. Rev. C **44**, 1296 (1991).

[25] M. Jetter, H. Freitag, and H. V. von Geramb, Nucl. Phys. **A553**, 665c (1993).

[26] A. Katsogiannis and K. Amos, Phys. Rev. C **47**, 1376 (1993).

[27] W. F. Ford, Phys. Rev. **133**, B1616 (1964).

[28] W. F. Ford, J. Math. Phys. **7**, 626 (1966).

[29] M. R. C. McDowell and J. P. Coleman, *Introduction to the Theory of Ion-Atom Collisions*, North-Holland Publishing Company, Amsterdam (1970).

[30] J. Zorbas, J. Math. Phys. **17**, 498 (1976).

[31] J. Zorbas, J. Math. Phys. **18**, 1112 (1977).

[32] B. Talukdar, D. K. Gosh, T. Sasakawa, J. Math. Phys. **23**, 1700 (1982); B. Talukdar and D. K. Gosh, *Few Body Problems in Physics, ed.* B. Zeitnitz, North-Holland Publishing

Company, Amsterdam (1984).

[33] J. Dušek, Czech. J. Phys. B **31**, 941 (1981).

[34] J. Dušek, Czech. J. Phys. B **32**, 1325 (1982).

[35] M. Gell-Mann and M. L. Goldberger, Phys. Rev. **91**, 398 (1953).

[36] M. G. Fuda and J. S. Whiting, Phys. Rev. C **8**, 1255 (1973).

[37] H. P. Stapp, T. J. Ypsilantis, and N. Metropolis, Phys. Rev. **105**, 302 (1957).

[38] J. M. Blatt and L. C. Biedenharn, Phys. Rev. **86**, 399 (1952).

[39] H. van Haeringen and R. van Wageningen, J. Math. Phys. **16**, 1441 (1975).

[40] M. G. Fuda, Phys. Rev. C **14**, 37 (1976).

[41] A. Nordsieck, Phys. Rev. **93**, 785 (1954).

[42] S. Okubo and D. Feldman, Phys. Rev. **117**, 292 (1960).

[43] Ch. Elster, L. C. Liu, and R. M. Thaler, Los Alamos National Laboratory Report LA-UR-90-2126, 1990.

[44] J. M. J. van Leeuwen and A. S. Reiner, Physica **27**, 99 (1961).

[45] M. Jetter, *Nukleon-Nukleon und Nukleon-Antinukleon Bremsstrahlung im Potentialmodell*, PhD thesis, University of Hamburg, 1993.

[46] C. A. Smith, J. V. Jovanovich, and L. G. Greeniaus, Phys. Rev. C **22**, 2287 (1980); L. G. Greeniaus *et al*, Phys. Rev. Lett. **35**, 696 (1975).

[47] J. V. Jovanovich, L. G. Greeniaus, J. McKeown, T. W. Millar, D. G. Peterson, W. F. Prickett, K. F. Suen, and J. C. Thompson, Phys. Rev. Lett. **26**, 277 (1971).

FIGURES

Fig. 1. The 5 MeV $pp\gamma$ photon cross section (left) and analyzing powers (right) for proton scattering angles of 30° (top), 12° (middle), and 5° (bottom). The results of calculations made using the 'full Coulomb', 'no Coulomb', 'simple Coulomb', and 'on-shell Coulomb' prescriptions are displayed by the solid, dotted, dashed, and dot-dashed curves respectively.

Fig. 2. Same as Fig. 1 but for 42 MeV. Data are taken from Ref. [47].

Fig. 3. Same as Fig. 1 but for 157 MeV and $\bar{\phi} = 0.5°$ for the top panels. Data are taken from Ref. [7].

Fig. 4. The photon cross section data from 157 MeV $pp\gamma$ in the 'Harvard Noncoplanar Geometry' [13] for (30°, 30°) with diverse noncoplanar angle, $\bar{\phi}$. The solid, dashed, and dotted curves give the results with $\bar{\phi}$ being 0°, 0.5°, and 1.0° respectively. The dot-dashed curve is the $\bar{\phi} = 0.5°$ result when rescattering terms are neglected. Data are taken from Ref. [7].

Fig. 5. The coplanar 280 MeV $pp\gamma$ photon cross section (left) for proton scattering angles (θ_1, θ_2)= (27.8°, 28°) (top), (12.4°, 12°) (middle), and (5°, 5°) (bottom), where θ_2 is for the 'low- energy proton', detected on the same side of the beam line as the photon. The analogous analyzing powers are shown on the in the right panels except that for the middle panel (θ_1, θ_2)= (12.4°, 14°). The results of calculations made using the 'full Coulomb', 'no Coulomb', 'simple Coulomb', and 'on-shell Coulomb' models are displayed by the solid, dotted, dashed, and dot-dashed curves respectively. Data are taken from Ref. [16].

Fig. 6. The 280 MeV analyzing power for (12.4°, 14°) coplanar geometry. The 'full Coulomb' results with and without rescattering terms are represented by the solid and dashed curves respectively. The 'on-shell Coulomb' prescription with and without rescattering terms gave the results displayed by the dot-dashed and dotted curves respectively. Data are taken from Ref. [16].

Fig. 7. The coplanar (5°, 5°) photon cross sections calculated with the 'full Coulomb' model and for 5 MeV (solid), 42 MeV (dashed), 157 MeV (dot-dashed), and 280 MeV (dotted).

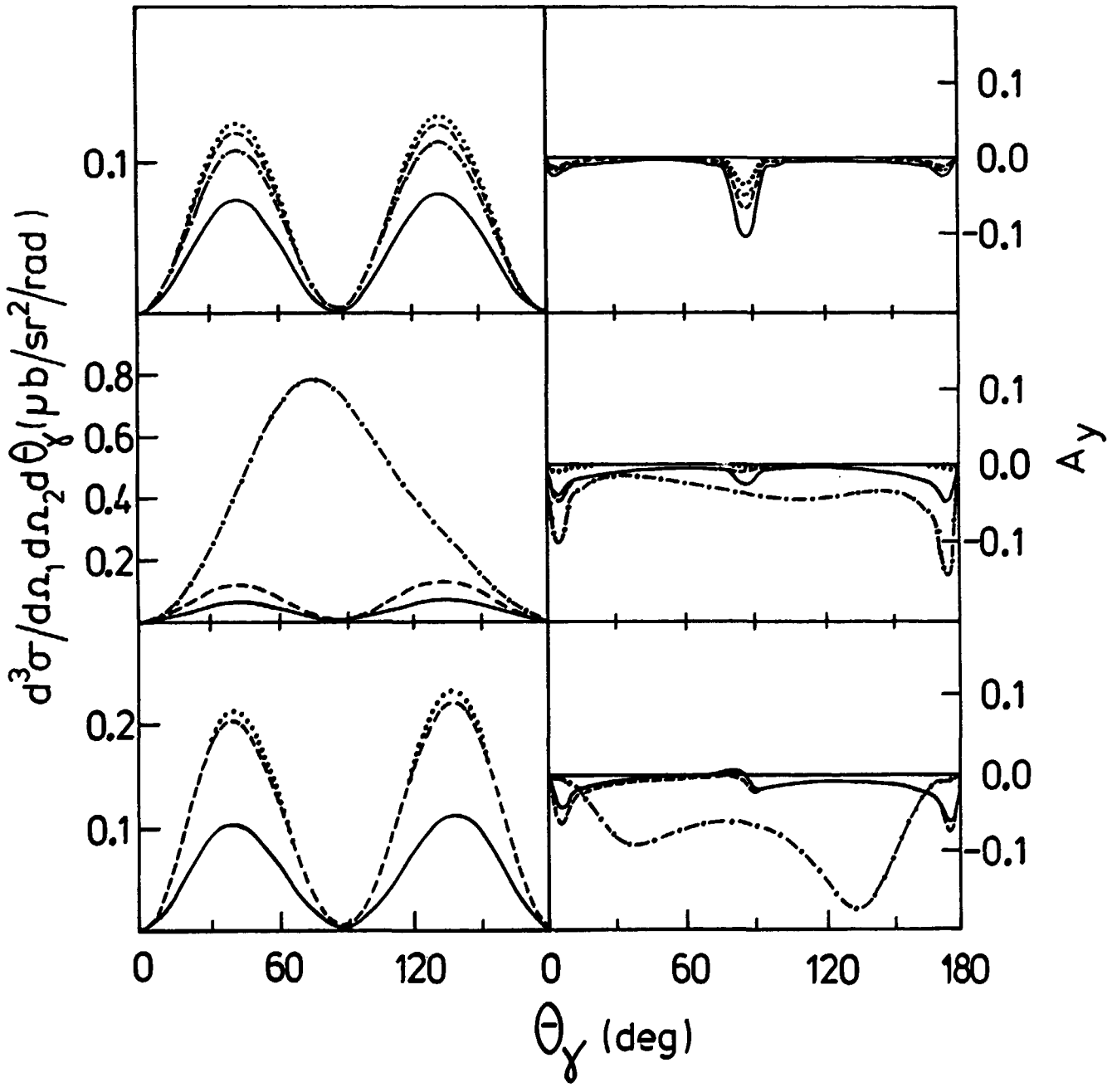
$d^3\sigma/d\Omega_1 d\Omega_2 d\Theta_\gamma$ (μb/sr²/rad)
0.1
0.8
0.6
0.4
0.2
0.2
0.1
0.1
0.0
-0.1
0.1
0.0
-0.1
0.1
0.0
-0.1
A_y
0
60
120
0
60
120
180
Θ_γ (deg)

Fig. 1

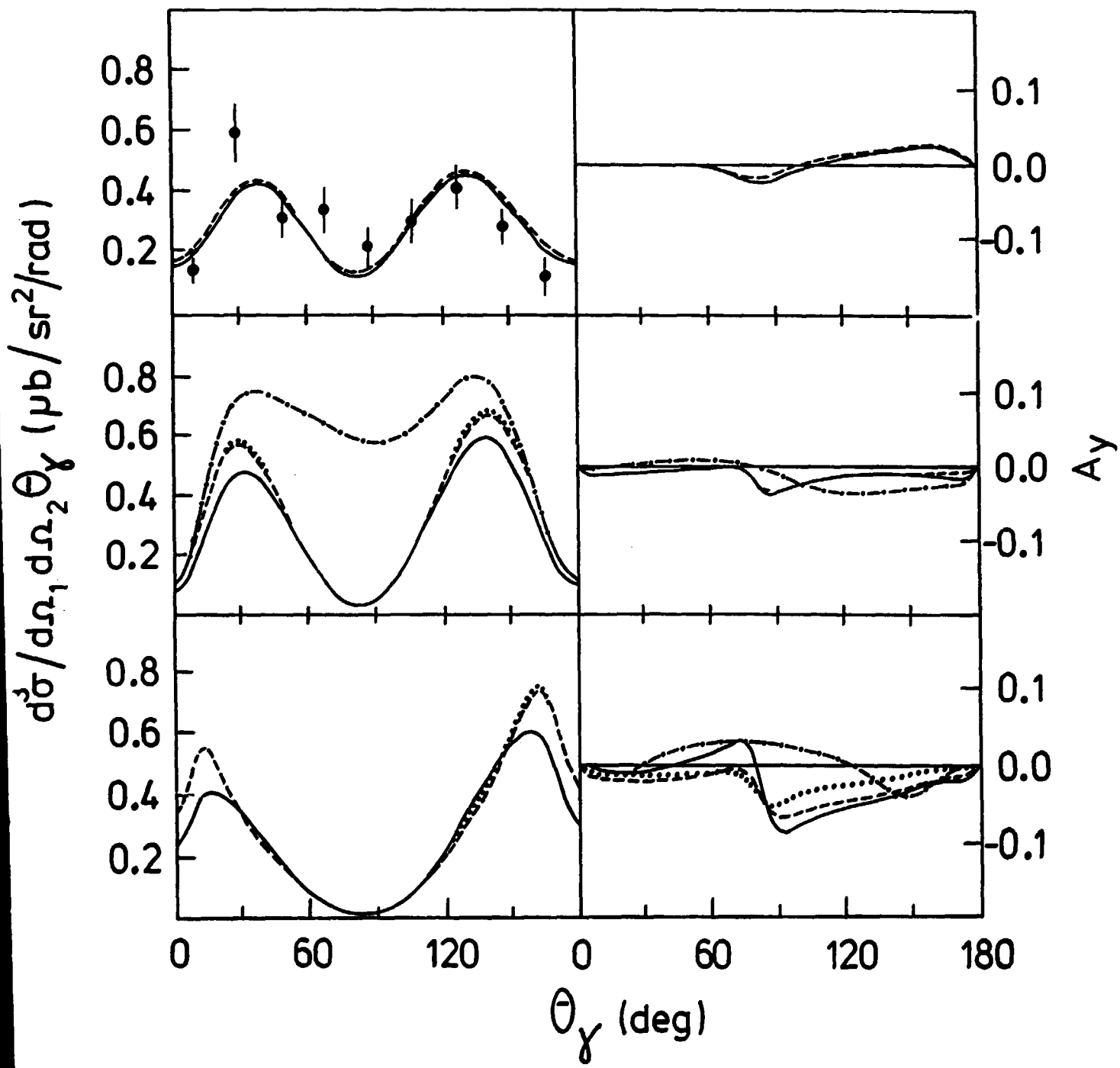
0.8
0.6
0.4
0.2
0.1
0.0
-0.1
Ay
0
60
120
180
$d^3\sigma/d\Omega_1 d\Omega_2 \Theta_\gamma$ (μb/sr²/rad)
Θ_γ (deg)

Fig. 2

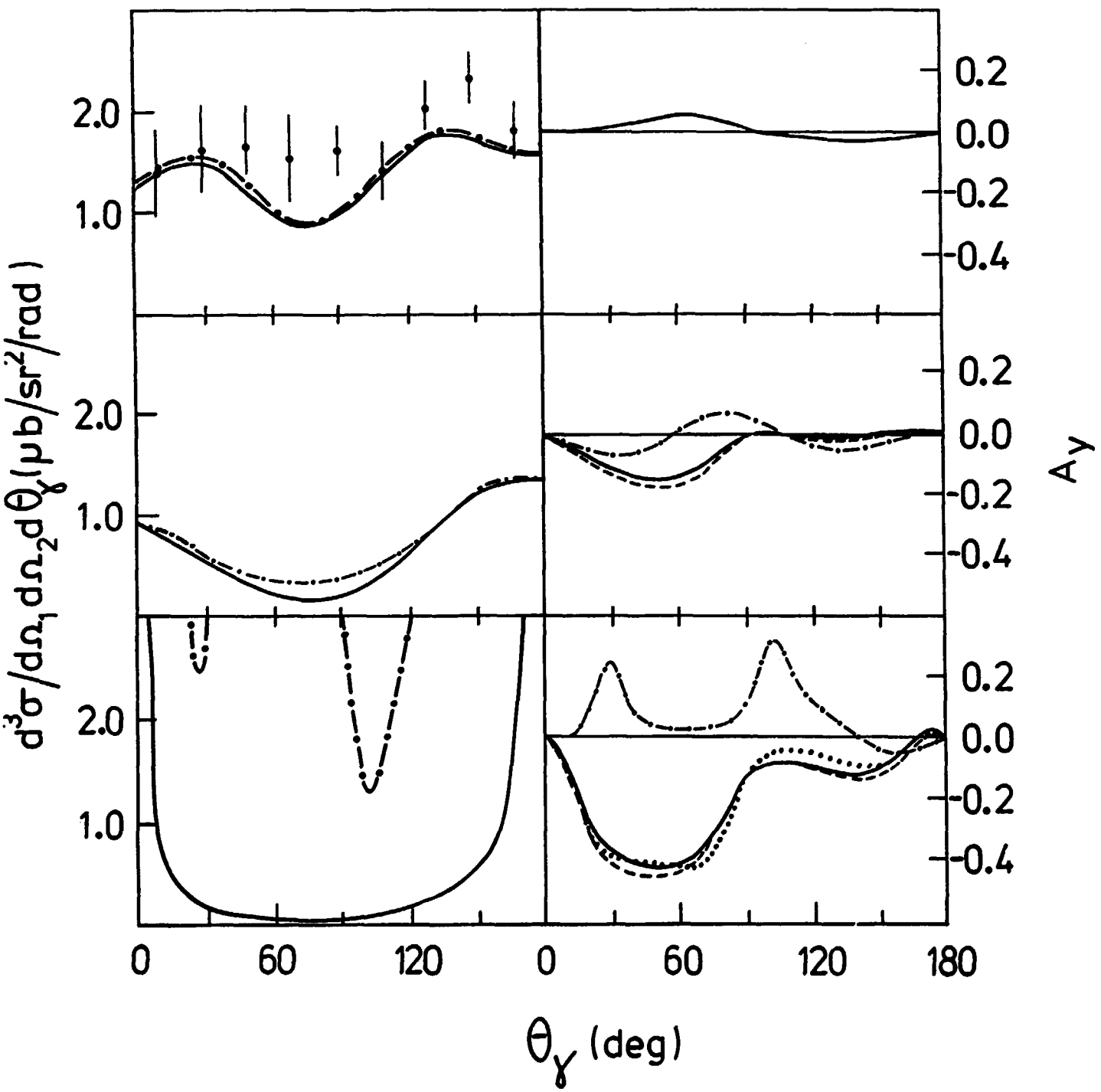
2.0
1.0
0.2
0.0
-0.2
-0.4
$d^3\sigma/d\Omega_1 d\Omega_2 d\theta_\gamma (\mu b/sr^2/rad)$
A_y
0
60
120
180
θ_γ (deg)

Fig. 3

3.0
2.0
1.0
0
30
60
90
120
150
180
$d^3\sigma/d\Omega_1 d\Omega_2 \Theta_\gamma$ (μb/sr²/rad)
Θ_γ (deg)

Fig. 4

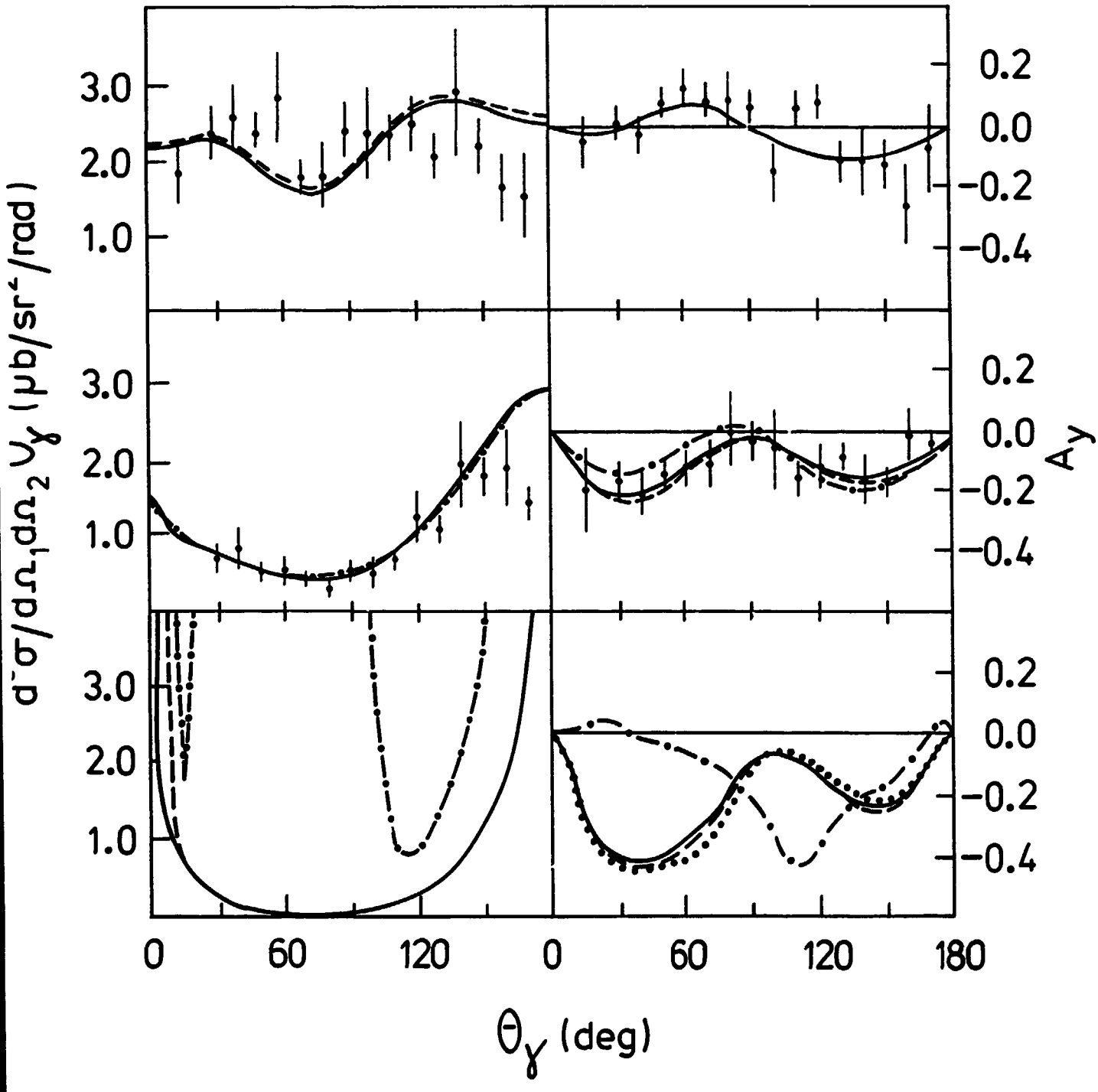
3.0
2.0
1.0
0.2
0.0
−0.2
−0.4
0
60
120
180
$d^2\sigma/d\Omega_1 d\Omega_2 V_\gamma$ (μb/sr²/rad)
A_y
Θ_γ (deg)

Fig. 5

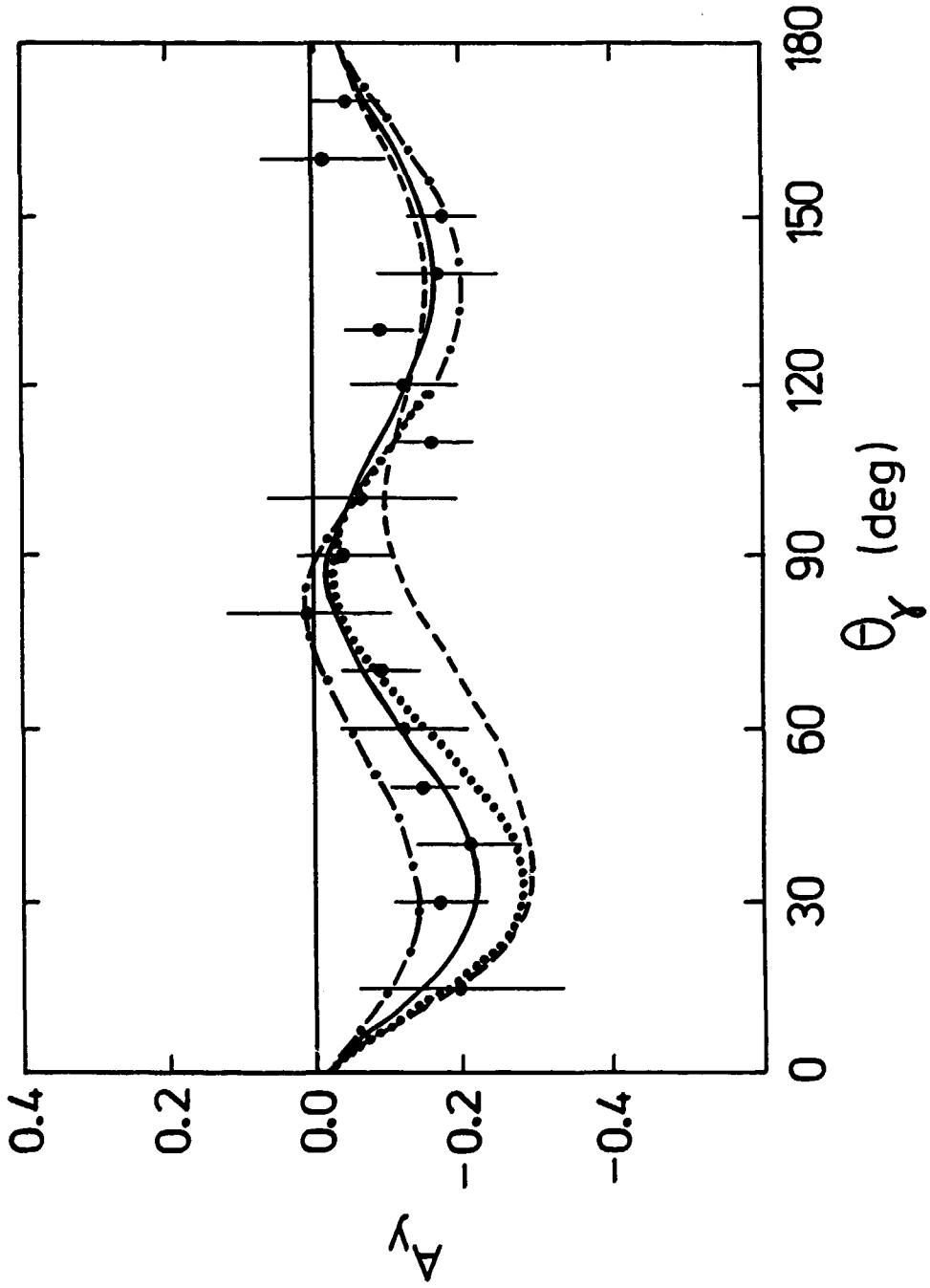

Fig. 6

$d^3\sigma/d\Omega_1 d\Omega_2 d\Theta_\gamma$ (μb/sr²/rad)
10^{1}
10^{0}
10^{-1}
10^{-2}
0
30
60
90
120
150
180
Θ_γ (deg)

Fig. 7